# Research of b-Value of the Global Plate Subduction Zone based on Weibull Distribution

Jie YU[1],Zhi-yao LI[1]*,Shuang YU[2],Tian-tian XU[1]
[1]Mechanical Engineering College of Changchun University, CHINA
[2]Foreign Trade Department of Changchun Vocational and Technical College, CHINA

**Abstract:** B-value curves and Amira images of the global plate subduction zones have been drawn and the parameters of Weibull Distribution have been calculated. The relationship diagrams of B-values and the parameters of Weibull Distribution of the whole subduction zones have been drawn.

**Keywords:** Weibull Distribution; B value; Earthquake; Subduction zone; Plate

## 1. Introduction

Subduction zone is the subduction parts of the subducting plate and lies in the range of the plates. Subduction zone is divided into two types which are type A and type B. Type A consists of continent-continent subduction zone and type B consists of ocean-ocean subduction zone. Type B subduction zone consists of huge Benioff zones which develop ditches, arcs and strong earthquakes and volcanic activities.

## 2. Temporal Clustering of Global Seismic Image

According to the seismic catalog which comes from USGS during 1st. Jan. 1973 and 14th. July 2011, we get 300440 earthquakes above level 4.0 and we draw the temporal clustering of global seismic image. X-axis shows the subduction zones and Y-axis shows the time. Different earthquake levels show with different color balls. Blue balls show the levels from 4.0 to 4.9. Green balls show the levels from 5.0 to 5.9. Pink balls show the levels from 6.0 to 6.9. Yellow balls show the levels from 6.0 to 6.9. Red balls show the levels above 8.0.

From Fig.1 we can see that the global subduction zones consisting of several main seismic clustering and the central pacific plates cluster intensive earthquakes and the central pacific zones often earthquake and erupt frequently. There are a series of trenches, islands and volcanoes on the central pacific plates with violent plate movements. Alpine-Himalayan belt is clustered earthquakes where are mainly east-west huge mountains across the central and southern Eurasia and northern Africa.

The earthquakes are also active in mid-Atlantic ridge extending south-north of the Pacific ocean which lies in the middle of the ocean basin and extends to the series of mainland shore between flat abyssal plains. Fig.2 is the 3D image of the global catalog with the depth. From the depth, we can see that the earthquakes cluster intensively around the east ridge and the west ridge of the Pacific plates and distribute widely in the depth.

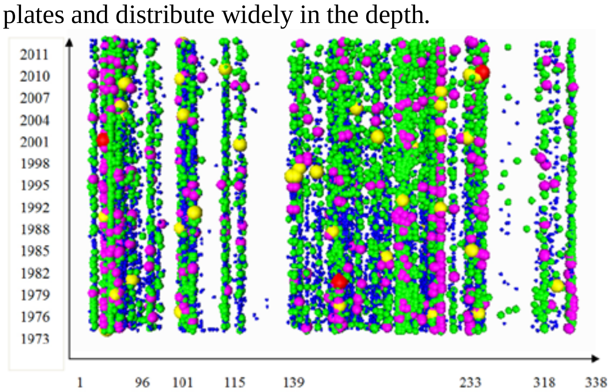


**Figure 1. Temporal Clustering of Global Seismic Image**

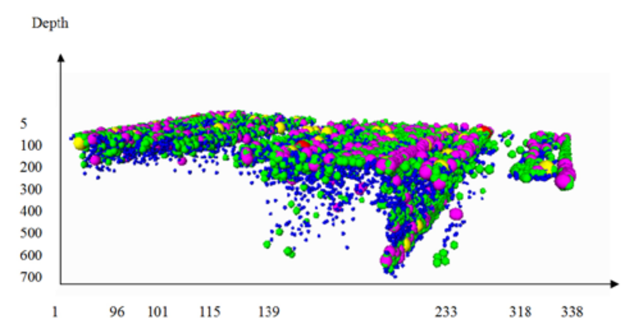


**Figure 2. 3D image of the global catalog with the depth**

The seismic catalog of the whole Pacific seismic belt, Eurasian seismic zone and Ridge earthquake belt show the obvious earthquake cluster properties in terms of time and space. Therefore, we can get the main activity properties of the main plate belts of the whole global from the probability and statistics. With the supplement and improvement of the seismic catalog, we can adopt the Visualization of the earthquake clusters and Weibull distribution to estimate the distribution of precursor of the main seismic initially which can be used as the seismic prediction.

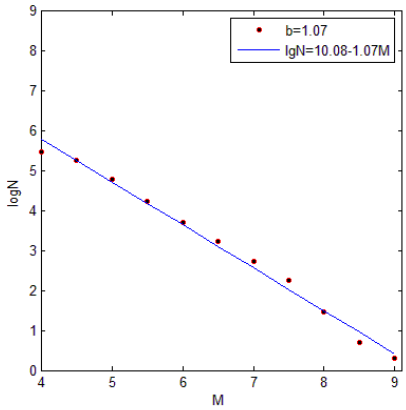


**Figure 3. B-value curve of the global catalog ( limit level:4.0)**

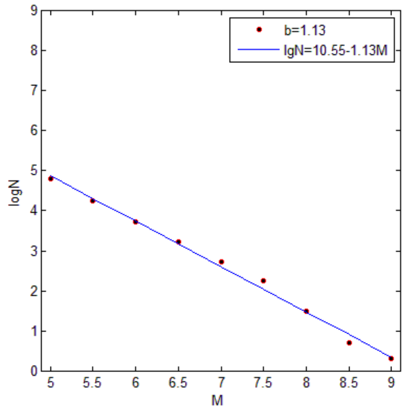


**Figure 4. B-value curve of the global catalog ( limit level:5.0)**

From Fig.3 and Fig.4 we can see that the fitting curves have no data dots belowing the fitting lines. We can draw the results that the seismic catalog records above level 4 and level 5 are complete. These data provide a reliable basis for the following statistic analysis.

Weibull parameters of the global catalog are given as below: $\hat{k}=1.110, \hat{b}=12$ (t=463m).

## 3. B-value Analysis Based on Weibull Distribution of the Global Plate Subduction Zone

We divide the global plate subduction zone into 338 parts. For the parts with no records, we don't analyze. For some seismic zones, we can't draw b-value curves because the earthquake levels below 5.0. The data are also from USGS during 1st. Jan. 1973 and 14th. July 2011.

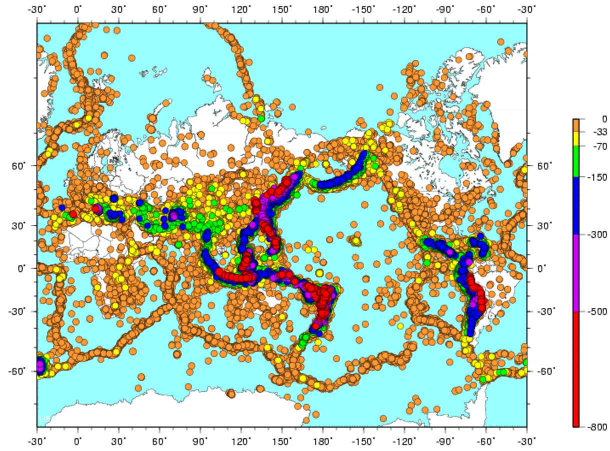


**Figure 5. The global seismic map (1/1/1973-7/14/2011)**

We select representative subduction zones and draw b-value curves and 3D images and calculate Weibull parameters. We analyze the physical meanings of the fault zones.

Subduction 10 (Longitude:142-180, Latitude:60-51): b-value curve and 3D image are given as below:

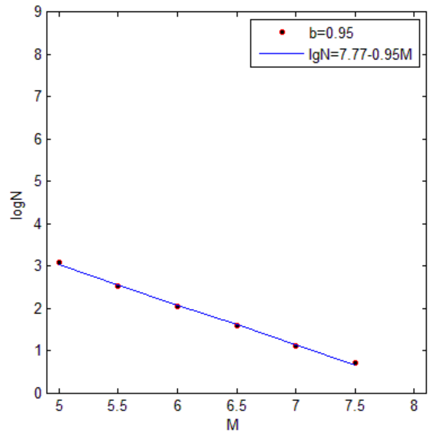


**Figure 6. B-value of subduction 10**

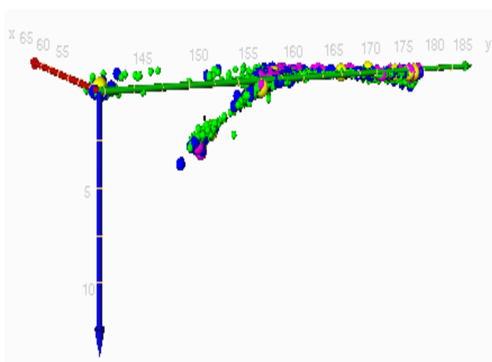

**Figure 7. 3D image of subduction 10**

We get Weibull parameters of subduction 10: $\hat{k}=1.05, \hat{b}=114.31$.

Subduction 104 (Longitude: 120.57-126.31, Latitude: 23.79-26.39): b-value curve and 3D image are given as below:

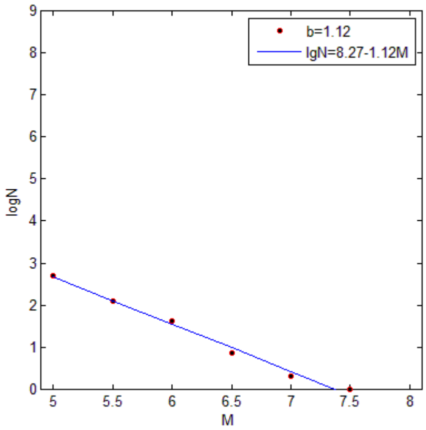


Figure 8. B-value of subduction 104

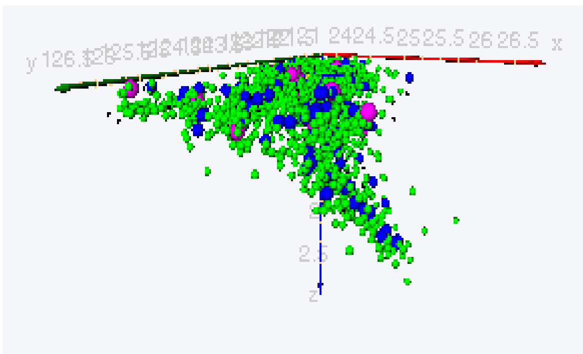

Figure 9. 3D image of subduction 104

We get Weibull parameters of subduction 104: $\hat{k}=1.10, \hat{b}=105.35$.

Subduction 177 (Longitude: 118.93-135.18, Latitude: 12.52-3.05): b-value curve and 3D image are given as below:

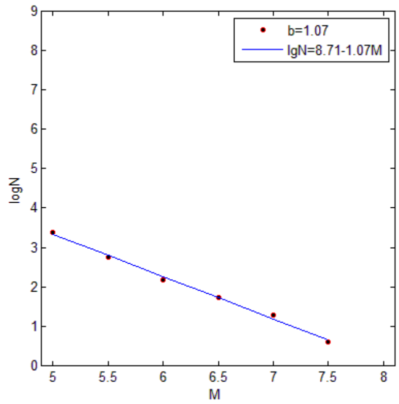


Figure 10. B-value of subduction 177

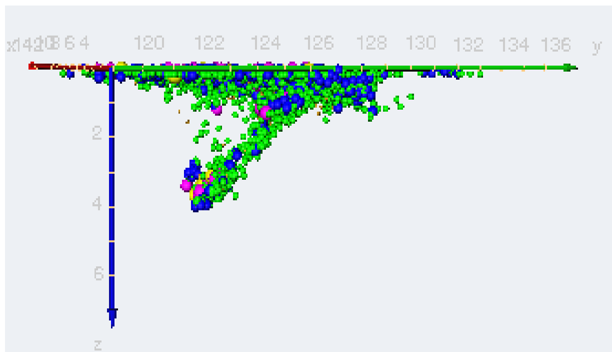

Figure 11. 3D image of subduction 177

We get Weibull parameters of subduction 177: $\hat{k}=1.03, \hat{b}=105.09$

## 4. Weibull Distribution Parameters of the Subduction Zones

The paper can't list b-value curves and 3D images of all the subduction zones because of limited space. We calculate all Weibull Distribution parameters listed in table 1( we can't list the subduction zones without earthquake or incomplete data).

Table 1. Weibull Distribution Parameters and b-values

| Subduction number | Longitude | Latitude | b-value | Weibull Distribution Parameters $\hat{b}$, $\hat{k}$ (t=461m) |
|---|---|---|---|---|
| 2 | 70.6-82.7 | 20.6-17.8 | 0.30 | $\hat{k}=1.69, \hat{b}=140.02$ |
| 3 | 114-125 | 41-32 | 0.57 | $\hat{k}=1.42, \hat{b}=138.22$ |
| 4 | 31-47 | 38-14 | 1.06 | $\hat{k}=1.07, \hat{b}=117.05$ |
| 5 | 21-33 | 65-36 | 0.82 | $\hat{k}=1.16, \hat{b}=121.01$ |
| 8 | 123-131 | 52-39 | 0.34 | $\hat{k}=1.67, \hat{b}=138.02$ |
| 10 | 142-180 | 60-51 | 0.95 | $\hat{k}=1.05, \hat{b}=114.31$ |
| 11 | 99-107 | 22-15 | 0.46 | $\hat{k}=1.55, \hat{b}=136.32$ |
| 12 | 107-116 | 34-20 | 1.69 | $\hat{k}=1.65, \hat{b}=137.88$ |

| | | | | |
|---|---|---|---|---|
| 13 | 57-83 | 11-0 | 1.72 | $\hat{k}$=1.77,$\hat{b}$=140.62 |
| 14 | 19.0-10.0 | 56-5 | 1.29 | $\hat{k}$=1.30,$\hat{b}$=120.22 |
| 15 | 33-77 | 56-50 | 1.91 | $\hat{k}$=1.89,$\hat{b}$=141.21 |
| 20 | 70-83 | 52-4.0 | 1.03 | $\hat{k}$=1.01,$\hat{b}$=108.58 |
| 24 | 94-101 | 17-14 | 1.32 | $\hat{k}$=1.33,$\hat{b}$=116.33 |
| 26 | 76-83 | 19-16 | 0.48 | $\hat{k}$=1.53,$\hat{b}$=135.62 |
| 27 | 74-78 | 19-16 | 0.48 | $\hat{k}$=1.53,$\hat{b}$=135.61 |
| 28 | 77-88 | 11-5 | 0.80 | $\hat{k}$=1.21,$\hat{b}$=113.18 |
| 29 | 58-68 | 20-9 | 0.81 | $\hat{k}$=1.21,$\hat{b}$=113.16 |
| 36 | 72-77 | 19-17 | 1.69 | $\hat{k}$=1.65,$\hat{b}$=137.16 |
| 37 | 70-75 | 19-17 | 1.69 | $\hat{k}$=1.65,$\hat{b}$=137.16 |
| 38 | 70-74 | 21-17 | 1.81 | $\hat{k}$=1.76,$\hat{b}$=141.02 |
| 43 | 0-19 | 74-66 | 1.53 | $\hat{k}$=1.55,$\hat{b}$=135.22 |
| 63 | 143-151 | 44-40 | 0.89 | $\hat{k}$=1.11,$\hat{b}$=109.28 |
| 64 | 0-24 | 38-35 | 0.93 | $\hat{k}$=1.09,$\hat{b}$=108.36 |
| 65 | 17-26 | 40-33 | 0.83 | $\hat{k}$=1.15,$\hat{b}$=111.82 |
| 66 | 24-30 | 37-33 | 1.21 | $\hat{k}$=1.22,$\hat{b}$=118.02 |
| 67 | 65-71 | 34-24 | 1.09 | $\hat{k}$=1.05,$\hat{b}$=106.65 |
| 68 | 69-97 | 36-26 | 0.97 | $\hat{k}$=1.04,$\hat{b}$=106.01 |
| 69 | 92-97 | 28-19 | 0.99 | $\hat{k}$=1.01,$\hat{b}$=100.02 |
| 70 | 57-67 | 26-12 | 1.17 | $\hat{k}$=1.15,$\hat{b}$=111.26 |
| 71 | 36-43 | 39-36 | 1.05 | $\hat{k}$=1.06,$\hat{b}$=106.09 |
| 72 | 33-38 | 38-26 | 0.86 | $\hat{k}$=1.25,$\hat{b}$=119.67 |
| 189 | 124.93-130.06 | 124.93-130.06 | 1.26 | $\hat{k}$=1.28,$\hat{b}$=115.50 |
| 190 | 128.08-134.68 | 6.44-1.43 | 1.24 | $\hat{k}$=1.27,$\hat{b}$=115.39 |
| 191 | 124.47-128.14 | 8.76-6.33 | 0.96 | $\hat{k}$=1.04,$\hat{b}$=105.86 |
| 192 | 147.84-150.55 | 4.10-0 | 0.70 | $\hat{k}$=1.30,$\hat{b}$=119.72 |
| 193 | 142.49-146.64 | 7.28-4.68 | 0.6 | $\hat{k}$=1.37,$\hat{b}$=116.83 |
| 194 | 118.91-124.8 | 14.98-11.16 | 0.97 | $\hat{k}$=1.02,$\hat{b}$=100.37 |
| 196 | 137.56-147.06 | 10.03-5.51 | 0.94 | $\hat{k}$=1.03,$\hat{b}$=100.39 |
| 197 | 120.0-122.58 | 25.18-21.81 | 0.96 | $\hat{k}$=1.01,$\hat{b}$=99.39 |
| 198 | 118.35-121.1 | 20.82-12.46 | 1.17 | $\hat{k}$=1.11,$\hat{b}$=108.55 |
| 199 | 140.99-144.2 | 35.31-25.17 | 1.32 | $\hat{k}$=1.32,$\hat{b}$=116.00 |
| 200 | 137.17-142.99 | 36.26-32.88 | 1.33 | $\hat{k}$=1.32,$\hat{b}$=115.82 |
| 201 | 126.13-138.21 | 2.79-0 | 1.17 | $\hat{k}$=1.15,$\hat{b}$=111.35 |
| 202 | 131.82-144.77 | 4.39-0 | 0.86 | $\hat{k}$=1.15,$\hat{b}$=111.65 |
| 203 | 131.82-147.99 | 4.21 -0 | 0.89 | $\hat{k}$=1.12,$\hat{b}$=110.05 |
| 204 | 142.77-147.99 | 4.39 -2.21 | 0.60 | $\hat{k}$=1.43,$\hat{b}$=138.43 |
| 205 | 130.37-136.84 | 2.38 -0 | 0.86 | $\hat{k}$=1.15,$\hat{b}$=111.00 |

| | | | | |
|---|---|---|---|---|
| 206 | 141.57-145.21 | 12.82 -10.71 | 1.25 | $\hat{k}$=1.23,$\hat{b}$=118.67 |
| 207 | 139.93-141.24 | 11.99 -9.96 | 1.15 | $\hat{k}$=1.13,$\hat{b}$=109.75 |
| 208 | 140.65-148.88 | 27.17 -10.08 | 1.05 | $\hat{k}$=1.06,$\hat{b}$=106.72 |
| 209 | 141.27-145.87 | 23.57 -10.83 | 0.98 | $\hat{k}$=1.02,$\hat{b}$=108.63 |
| 210 | 42.65-55.15 | 15.77 -11.01 | 1.10 | $\hat{k}$=1.09,$\hat{b}$=109.02 |
| 211 | 53.19-55.25 | 15.71 -13.69 | 1.87 | $\hat{k}$=1.83,$\hat{b}$=139.05 |
| 212 | 53.29-55.33 | 15.68 -13.67 | 1.87 | $\hat{k}$=1.83,$\hat{b}$=139.03 |
| 213 | 53.39-57.18 | 15.87 -13.64 | 2.79 | $\hat{k}$=1.96,$\hat{b}$=150.06 |
| 214 | 55.21-59.13 | 15.64 -11.83 | 1.27 | $\hat{k}$=1.21,$\hat{b}$=117.52 |
| 215 | 55.92-59.13 | 13.83 -8.86 | 1.13 | $\hat{k}$=1.15,$\hat{b}$=110.51 |
| 216 | 56.03-71.09 | 26.64 -0 | 1.05 | $\hat{k}$=1.03,$\hat{b}$=107.55 |
| 217 | 64.01-70.85 | 26.64 -5.82 | 0.59 | $\hat{k}$=1.48,$\hat{b}$=139.05 |
| 218 | 31.97-46.14 | 16.26 -4.64 | 1.13 | $\hat{k}$=1.12,$\hat{b}$=109.36 |
| 221 | 136.23-148.80 | 7.40 -0.80 | 0.64 | $\hat{k}$=1.38,$\hat{b}$=117.72 |
| 222 | 136.23-148.80 | 7.40 -0.80 | 1.06 | $\hat{k}$=1.00,$\hat{b}$=97.37 |
| 223 | 149.72-163.77 | 63.73 -58.48 | 1.04 | $\hat{k}$=1.03,$\hat{b}$=107.39 |
| 224 | 18.99-70.96 | 54.47 -24.64 | 0.99 | $\hat{k}$=1.01,$\hat{b}$=97.33 |
| 225 | 0-20.99 | 55.86 -50.79 | 1.69 | $\hat{k}$=1.66,$\hat{b}$=137.62 |
| 228 | 161.77-180.93 | 66.61 -60.74 | 0.67 | $\hat{k}$=1.65,$\hat{b}$=137.36 |
| 230 | 165.93-168.29 | 64.64 -61.11 | 0.95 | $\hat{k}$=1.02,$\hat{b}$=100.61 |
| 231 | 150.44-164.63 | 64.22 -58.43 | 1.02 | $\hat{k}$=1.00,$\hat{b}$=97.42 |
| 232 | 54.28-76.99 | 62.41 -50.82 | 0.95 | $\hat{k}$=1.06,$\hat{b}$=110.05 |
| 318 | 109.39-152.44 | 35.60-30.56 | 0.97 | $\hat{k}$=1.00,$\hat{b}$=97.35 |
| 320 | 156.35-165.97 | 60.68-45.74 | 1.06 | $\hat{k}$=1.05,$\hat{b}$=109.27 |
| 321 | 158.74-163.77 | 62.74-58.68 | 1.20 | $\hat{k}$=1.25,$\hat{b}$=119.07 |
| 322 | 104.40-110.35 | 22.25-16.76 | 0.60 | $\hat{k}$=1.39,$\hat{b}$=118.03 |
| 327 | 123.47-131.53 | 47.35-39.31 | 0.39 | $\hat{k}$=1.60,$\hat{b}$=116.09 |
| 328 | 99.85-103.27 | 3.14-0 | 0.78 | $\hat{k}$=1.29,$\hat{b}$=115.37 |
| 338 | 74.54-110.05 | 47.37-33.11 | 0.94 | $\hat{k}$=1.05,$\hat{b}$=106.53 |

We draw the curves of shape parameters $\hat{k}$ and b-values of each subduction zones with horizontal direction of b-values and vertical direction of shape parameters $\hat{k}$ .

From Fig.12 we can see that $\hat{k}$ is always greater than 1.0 which are consistent to the unimodal state of the density function curve. When b-values change near 1.0, shape parameters also change near 1.0. For the subduction zones with large changes of b-values, shape parameters change obviously.

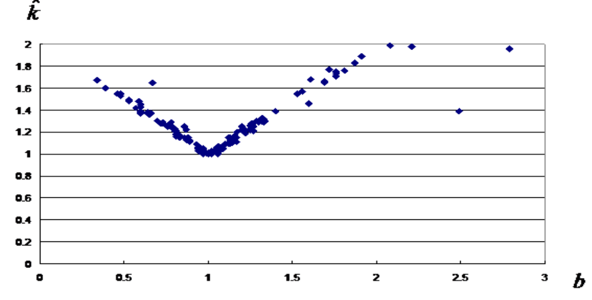


**Figure 12. B-values and shape parameters $\hat{k}$**

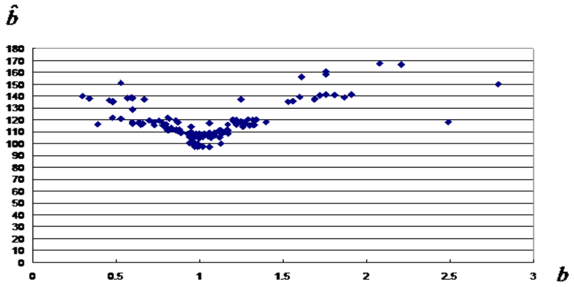


**Figure 13. B-values and shape parameters $\hat{b}$**

We draw the curves of scale parameters $\hat{b}$ and b-values of each subduction zones with horizontal direction of b-values and vertical direction of shape parameters $\hat{b}$ .

From Fig.13 we can see that scale parameters $\hat{b}$ are in fluctuating state with the changes of b-values.

## 5. Conclusions

The paper calculates b-values and draws the figures of b-values of the subduction zones. The paper draws 3D images of typical subduction zones and calculates parameters of Weibull distribution of the subduction zones with enough data.

For the further relationship of Weibull distribution parameters and b-values, we'll carry out in the following research.

## 6. Acknowledgement

This research work was sponsored by the project of Department of Education of Jilin Province (2015-LY-5-01-L05).

## References

[1] Chui-hong Fan. Applying Weibull Distribution function to earthquake prediction of Yishu fault. Northeast Earthquake Research. 1995.11(1):p59-67.

[2] Hua-chen Duan. Chang-qing Fan. Yue-min Xu. The calculation of b-value and the application in earthquake prediction. Earthquake Journal. 1995.17(4):p487-492.

[3] Xue-zhong Chen. Xiao-jian Lv. Hui-min Wang. B value of the seismically active and quiescent periods and research of seismicity tendency in China's continent. Earthquake.2001.1:p59-62.

[4] Yi Gui-xi, Wen Xue-ze. Earthquake recurrence on whole active fault zones and its relation to that on individual fault-segments. ACTA SEISMOLOGICA SINICA, 2000. 13(5): p. 563-574.

[5] Yi Gui-xi, Wen Xue-ze. Earthquake recurrence on whole active fault zones and its relation to that on individual fault-segments. ACTA SEISMOLOGICA SINICA, 2000. 13(5): p. 563-574.